POAC'25
St. John's, Newfoundland and Labrador, Canada

Proceedings of the 28th International Conference on Port and Ocean Engineering under Arctic Conditions
Jul 13-17, 2025
St. John's, Newfoundland and Labrador
Canada

Augmentation of Onboard Camera Data with Ship Manoeuvrability for Tactical Navigation Support in Ice

Mordecai Chimedza[1], Thomas Browne[2], Rocky Taylor[1]

[1] Memorial University of Newfoundland, St. John's, NL, Canada

[2] National Research Council of Canada, St. John's, NL, Canada

ABSTRACT

Shipping in Canadian Arctic waters involves significant risks, primarily due to potential ice interactions. To address these challenges, various support tools have been developed to enhance safe navigation in ice-prone regions. These include POLARIS, a system which evaluates vessel suitability for specific ice conditions, and onboard cameras, which act as sensors to capture and monitor ice conditions around a vessel. This study examines the effectiveness of these two decision support tools, emphasizing the need to account for operational parameters such as vessel speed and physical characteristics like vessel length when assessing a ship's ability to navigate safely through ice.

Image processing techniques, including projective transformation or homography, are applied to convert onboard camera data into a top-down view, enabling augmentation of ship manoeuvrability parameters, specifically the stopping distance and turning circle parameters. Image rescaling is further employed to achieve a true-scale representation of distances within the field of view. Two sample vessel scenarios are analyzed to evaluate their manoeuvrability in a test case involving a 50m diameter ice hazard at 175m directly ahead of the vessel. The results demonstrate the critical role of vessel speed in stopping distance. The results also show the limitations of using onboard cameras for tactical navigational support, as well as highlighting the limits that POLARIS has in terms of accounting for differences in vessels within the same ice class but with different capabilities.

KEY WORDS: Ice Navigation, Ship Manoeuvrability, POLARIS, Onboard Cameras, Ice Hazard Avoidance, Ice Monitoring, Ship Performance

INTRODUCTION

The receding ice cover and the warming temperatures as highlighted by Biggs and Green (2023) in the Arctic region have motivated ongoing study and research of the potential use of northern shipping routes which would save costs by shortening the duration of travel in comparison to current routes, according to Kooij and Hekkenberg (2019). The presence of sea

ice hazards in this region, however, presents a significant challenge and has motivated the research and adoption of navigational support tools to help with transit in these regions as shown in works by Neville (2016), Ruiz De-Azua et al (2018) and Zhou (2023). Additionally, further motivations for improving shipping safety for such an sea ice environment through the development of autonomous systems as highlighted by Randell et al (2008) and Kooij (2019), has further strengthened the interest in these support tools. The tools discussed in this paper are the hazard indexing framework called POLARIS, and the use of shipborne cameras for onboard ice monitoring for tactical navigation.

POLARIS, which stands for Polar Operational Limit Assessment Risk Indexing System, is a decision support framework, introduced through the International Maritime Organization's Polar Code, which helps provide guidance to vessel operators based on the sea ice conditions being faced and the polar class or ice class of a vessel, as explained by Browne et al (2020) and Transport Canada (2019). The ice conditions are described in terms of the concentration and stage of development of ice while the polar class depends on the vessel's capabilities in withstanding impact from sea ice features such as pack ice as mentioned by Transport Canada (2019). This support tool provides useful information in terms of operational limits for vessels based on their polar class.

To illustrate a vessel's capability to avoid hazards, its manoeuvrability is characterized by using two parameters, turning circle (or radius) and stopping distance, as per the American Bureau of Shipping (ABS) Manoeuvrability Guideline (2017) document. The turning circle parameter describes the vessel's ability to perform a 90-degree full port-side or starboard turn at a given speed, while the stopping distance describes a vessel's ability to stop dead in the water from an initial vessel speed. To ensure that vessel-specific maneuverability is accurately represented, vessel-specific parameters are incorporated into the calculation of these maneuverability parameters.

This paper maps these parameters on images obtained from an onboard camera that have been transformed to a top-down view using a principle known as homography or projective transformation. This helps illustrate the influence that vessel physical and operational parameters have on manoeuvrability and the resulting ability to safely navigate in sea ice and will be a good source for further analysis.

BACKGROUND

In assessing the POLARIS decision support tool, it is useful to consider speed recommendations which will be used as inputs to calculate the manoeuvrability parameters. These speed recommendations are given by POLARIS based on the polar class of a given vessel and are meant to ensure safe operations. Table 1 below shows the various vessel Polar Classes and their corresponding operational capability in sea ice.

Table 1. The Polar Classification system for Polar Class vessels

Polar Class	Ice Description
PC1	Year round operation in all Polar Waters
PC2	Year round operation in moderate multi year ice conditions
PC3	Year round operation in second year ice, which may include multi year ice inclusions

PC4	Year round operation in thick first year ice, which may include old ice inclusions
PC5	Yea round operation in medium first year ice which may include old ice inclusions
PC6	Summer/autumn operation in medium first year ice, which may include old ice inclusions
PC7	Summer/autumn operations in thin first year ice which may include old ice inclusions

Based on the assigned ice class and prevailing ice conditions, the vessels will have different recommendations depending on the calculated POLARIS Risk Index Outcome value. Scenarios in which vessels are deemed to be operating under elevated operational risk are prescribed recommended speed limits for operations in ice. These are shown in Table 2.

Table 2. Speed limits for Polar Class vessels operating under elevated operational risk

Polar Class (PC)	Recommended Speed Limit
PC1	11 knots
PC2	8 knots
PC3-PC5	5 knots
Below PC5	3 knots

In the current study, these speed limits are used as inputs in illustrating the boundaries of the vessel's stopping distance and turning circle. This is determined by using the methodologies in the sections that follow which include the calculation of the manoeuvrability parameters, image transformation and image rescaling and augmentation.

Using the classification system, an example vessel is used to illustrate the principle of manoeuvrability boundaries. The Canadian Coast Guard Ship (CCGS) Amundsen is used for the illustration. This vessel is a polar icebreaker, classified as Canadian Arctic Class 3, which can be considered to correspond to Polar Class 3. As such, for this paper, the calculation for the manoeuvrability parameters for the Amundsen will consider the recommended speed limits for "PC3-PC5" (5 knots) and the more conservative "Below PC5" (3 knots) as shown in Table 2.

Footage gathered from onboard cameras on the Amundsen will be used. The stopping distance and turning circle boundaries will be placed on a top-down image of the sea ice field to showcase the extent of the sea ice field visible from an onboard camera. Figure 1 shows an image from the vessel which will be used as the main input.

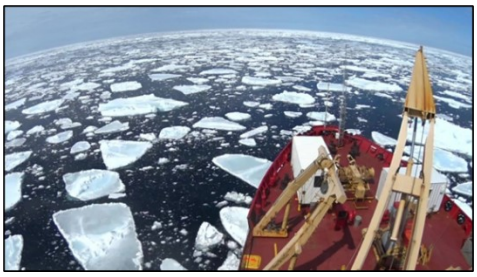

Figure 1. The initial image of the sea ice field from the onboard camera

RESEARCH METHODOLGY

To demonstrate the potential of mapping the boundaries of the stopping distance and turning circle parameters, several methodologies will be used. These will include the calculation of the manoeuvrability parameters, the image transformation process, and the image rescaling process. Finally, the image augmentation step will be carried out.

Manoeuvrability Parameter Calculations

The stopping distance is defined by a term known as the head reach, while the turning circle is defined by two values, the Advance and Transfer values. These two parameters are defined by the ABS Manoeuvrability Guideline (2017) and are determined through Stopping Distance and Turning Circle tests.

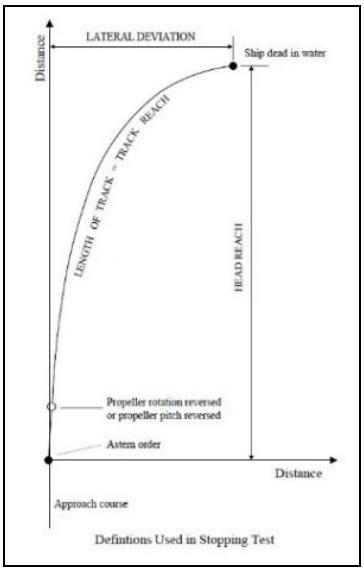

Figure 2. The Stopping Distance manoeuvrability test

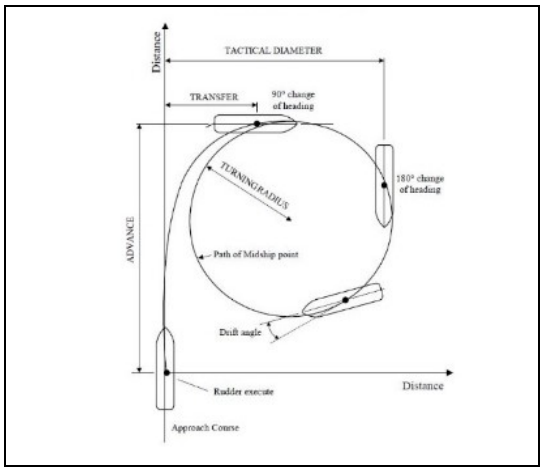

Figure 3. The Turning Circle manoeuvrability test

The corresponding parameters for these two tests can be calculated empirically using vessel specific properties.

First, the Stopping Distance can be calculated as follows:

$$S = \frac{(m+m_x)\cdot V_0^2}{2R_0} \cdot ln\left(1+\frac{R_0}{T_S}\right) + \frac{V_0 \cdot t_r}{2} \quad (1)$$

Where,

S is the stopping distance in m
m is the mass of the vessel,
m_x is the surge added mass (normally assumed to be 8% of vessel mass, [Sung et al])
V_0 is the approach speed of the vessel,
R_0 is the resistance of the vessel prior to the stopping maneuver,
T_S is the full astern thrust of the vessel, and
t_r is the time taken to reverse the shaft

Secondly, the Turning Circle can be calculated using the following equations:

$$\frac{Ad}{L} = 0.519\frac{TD}{L} + 1.33 \quad (2)$$

$$\frac{Tr}{L} = 0.497\frac{TD}{L} - 0.065 \quad (3)$$

Where,

TD is the Tactical Diameter in m,
L is the length in m,
STD is the steady turning diameter in m,
Vs is the test speed in knots,
Ad is the Advance in m and
Tr is the Transfer in m

In addition to the calculation of the corresponding parameters for the CCGS Amundsen vessel, the stopping distance and turning circle parameters will be calculated for various vessels to demonstrate the effect of vessel length on these calculations.

Image Transformation

Since onboard cameras are used in this study, one of the key objectives is the transformation and manipulation of the collected imagery data to obtain an image view that can be easily assessed and augmented with manoeuvrability parameters. This transformation involves the use of a principle called projective transformation, also known as homography.

Projective transformation is conducted by applying a matrix to the initial image so that it gives a transformed image as illustrated by Abbas et al (2019). This matrix is known as the homography matrix. The homography matrix is a transformation matrix that can be used to perform translation, rotation and warping transformations to other matrices. Since an image can be represented as a matrix with pixel values in its constituent locations, the homography

matrix can be applied to it to achieve the desired transformation.

The current study adopts this method to produce a top-down view of the sea ice field immediately ahead of the vessel. This allows for the image to be augmented with vessel manoeuvrability parameters.

To acquire the top-down view, a homography matrix is applied to the image. The homography matrix is determined from the camera specifications as well as some details of how the camera was positioned during the data collection. From first principles, the homography matrix can be determined by the following equation as highlighted by Dubrofsky (2009) and Sonka et al (2013):

$$H = K * R * K^{-1} \quad (4)$$

Where,

H is the homography matrix,
K is the camera intrinsic matrix and
R is the rotation matrix which represents image projective rotation.

The K matrix is the camera intrinsic matrix, and this is determined using the camera parameters according to Sandru et al (2020). These are obtained in the camera lens distortion removal process which can be carried out in MATLAB by performing a camera calibration.

$$K = \begin{pmatrix} \frac{fx}{Sx} & 0 & cx \\ 0 & \frac{fy}{Sy} & cy \\ 0 & 0 & 1 \end{pmatrix} \quad (5)$$

Where,

f_x is the focal length in the x direction,
S_x is the scaling factor length in the x direction,
f_y is the focal length in the y direction while
S_y is the scaling factor in the y direction; and
c_x and c_y are the coordinates of the image's optical centre

Image Rescaling

In addition to the transformation to a top-down view, the images also need to be scaled to reflect the true distance. This will help to ensure that the augmentation with the stopping distance and turning circle parameters will be accurate. This is carried out by applying varying scale factors to different pixels within an image. As is expected in the image shown in Figure 1, the size of objects in a picture reduces in comparison to objects of the same size that are closer to the image source (camera). In other words, the pixel to distance ratio changes as one moves deeper into the image and away from the camera.

The pixel to distance ratio changes became the basis for the methodology used to enlarge the image. Essentially, a scale factor would be applied to each pixel in the image to enlarge it based on its distance from the camera.

This process makes use of the known distance to a reference feature on the image and the distance to the horizon, which can be calculated using a generic equation. Finally, a correlation of the angle the camera makes with positions on the surface is related to the distance from the reference geometry to the horizon. Each increment in the angle is related to an increase in distance as one moves towards the horizon. A set of scale factors can be obtained which will then be used to enlarge the image to near true scale.

The process is outlined as a multi-step process as follows:

I. *Scaling and Reference Geometry*
II. *Distance to Horizon Calculation*
III. *Determining Relevant Camera Angles*
IV. *Discretization of Pixels in Region of Interest*

I.) *Scaling and Reference Geometry*

Firstly, a reference geometry of known dimensions and distance from the camera is identified in the image, along with the distance to the horizon. In this case, since the data used in this research was acquired several years ago (2015), physical measurements could not be taken. However, a feature of known geometry on the vessel itself was used (a shipping container, shown in Figure 4). Since schematic drawings of the Amundsen vessel were available, the full vessel length is known, and the true size of the reference geometry could be determined while its distance from the camera could also be estimated.

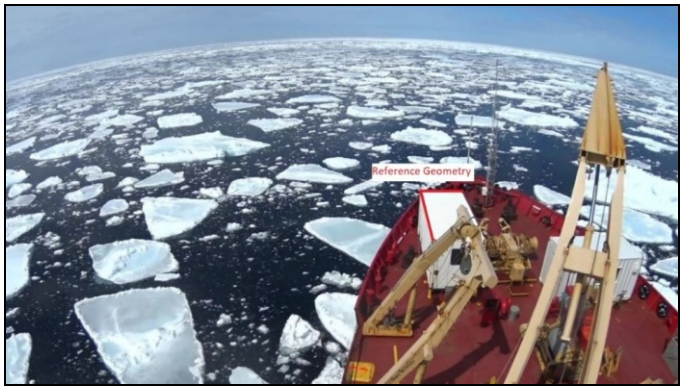

Figure 4. The labelled reference geometry used for image rescaling

II.) *Distance to Horizon Calculation*

Additionally, the distance to the horizon was also determined using a derived equation according to Imson (2005) which is the following:

$$D = \sqrt{(13 * H)} \tag{6}$$

Where,

D is the distance to the horizon in km and,
H is the height above sea level in m [73].

The distance from the camera to the horizon was noted for use in subsequent processing.

III.) Determining Relevant Camera Angles

A set of triangles are created to obtain the angles that the camera makes with reference geometry and the horizon. These are demonstrated in Figures 5 and 6.

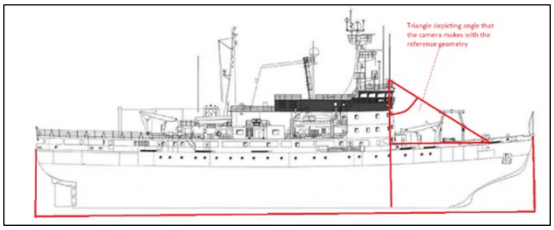

Figure 5. The camera angle to a reference geometry used for distance calculations

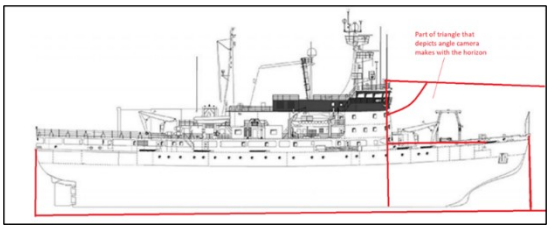

Figure 6. The camera angle to the horizon also used for sea ice field distance calculations

The distance between the edge of the reference geometry and the horizon is the region of interest and is the area that will be enlarged to show true scale.

IV.) Discretization of Pixels in Region of Interest

Once the angle range is determined, along with the distances of the reference edge and horizon from the camera, the image can be discretized to calculate the angle increment. This, in turn, defines the corresponding distance increment for each pixel step from the reference geometry to the horizon within the region of interest.

RESULTS AND DISCUSSION

Image Processing Results

The results from the calculations that were outlined in the previous section are described in this section. These include the results from the image processing steps, the transformations and the manoeuvrability parameter calculations. Additionally, the augmentation results of the transformed images with the manoeuvrability parameters are shown

The transformation of the image from a forward-looking view to a top-down view which can then be used for analysis is shown in Figure 7. Since the goal of the work is to augment the image with the vessel manoeuvrability parameters, the image needs to be in a perspective that would show the ocean surface plane.

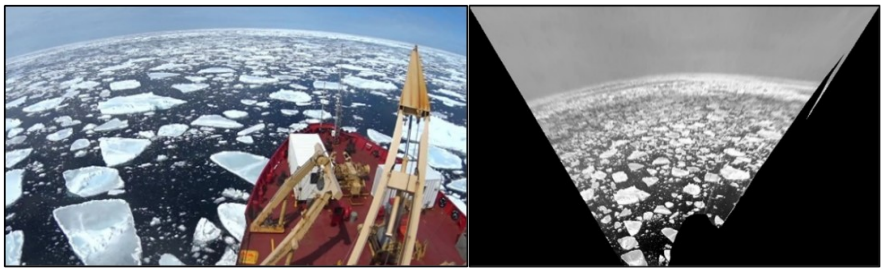

Figure 7. Transformed image (right) after processing steps compared to initial (left).

Manoeuvrability Results

The manoeuvrability results are shown in Table 3.

Table 3. Sample vessel manoeuvrability results for calculations at speeds of 5 and 3 knots

Parameter (ship lengths)	Speed of 5 knots	Speed of 3 knots
Vessel Length (m)	98	98
Stopping Distance	2.75	1.65
Advance	3.51	3.46
Transfer	2.02	1.97

In addition, the manoeuvrability parameters for other vessels used to show the effect of vessel length are also shown in Table 4.

Table 4. Sample vessel manoeuvrability results for different vessels at speeds of 5 knots

Parameter (m)	CCGS Amundsen (m)	Vessel 2 (m)	Vessel 3 (m)
Vessel Length	98	189	350
Stopping Distance	272	540	731
Advance	344	773	1008
Transfer	197	489	497

As can be seen, the general trend shows that for all the manoeuvrability parameters, their value increases as the length increases, highlighting the importance of accounting for the vessel length in the calculations of manoeuvrability and consequently, in sea ice hazard avoidance.

Image Rescaling and Augmentation with Manoeuvrability Parameters

Rescaling the image to reflect true size demanded a significant amount of computer memory and so a scale factor limit was applied, beyond which the scale factor was held constant but were still considered to be within an acceptable range. A scale factor upper limit of 30 was considered acceptable and selected as the upper limit for the image rescaling. Figure 8 shows the rescaled image with the scale factor limit of 30 applied, above which the scale factor is held constant.

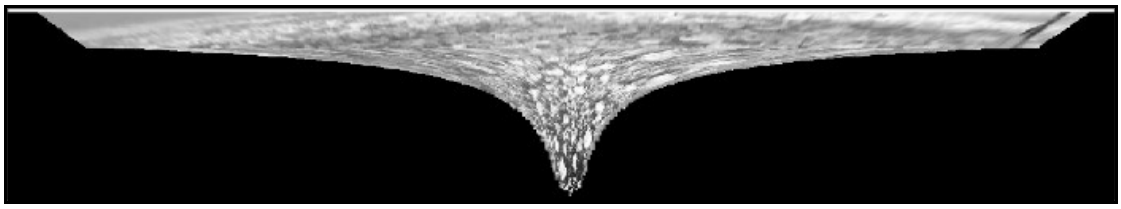

Figure 8. The rescaled image of the sea ice field

The next step was to see how this would relate to the operational boundaries of the vessel. The transformed and rescaled image was combined with the manoeuvrability parameters (turning circle and stopping distance). Two scenarios are considered where the vessel is sailing at 5 knots (Figure 9) and 3 knots (Figure 10). A fictional ice hazard that is 50 m in diameter and located 175 m directly ahead of the vessel is imposed on the images.

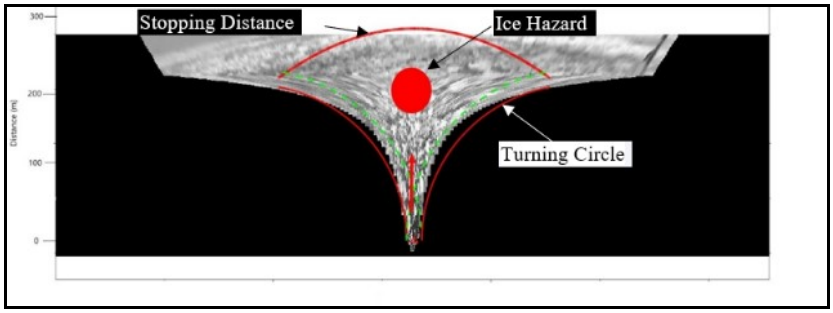

Figure 9. The augmentation results for vessel at speed recommendation of 5 knots

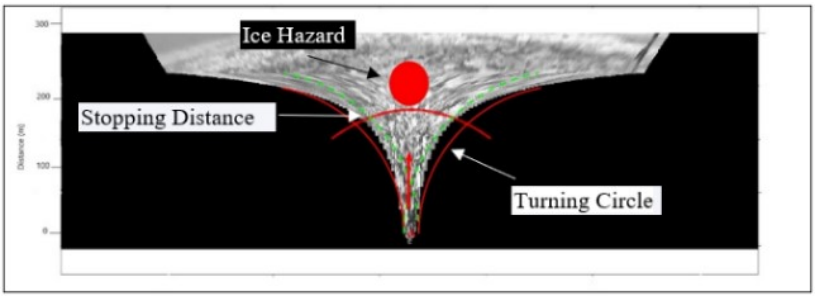

Figure 10. The augmentation results for the vessel at speed recommendation of 3 knots

Thus, based on the results obtained from the calculations and image processing steps, a few key observations were made. These included the following:

i. For both cases of vessel speeds of 5 and 3 knots, the turning circle parameters in Figures 9 and 10 appears to be wide enough to avoid the hazard. This suggests that turning would be a feasible method of hazard avoidance. It is worth noting, however, that this also depends on the width of the hazard and of the vessel.
ii. The stopping distance is insufficient for hazard avoidance in the 5 knots scenario while it is sufficient for a vessel that is travelling at 3 knots.
iii. Leading on from the previous point, it should be noted that the case study is the CCGS Amundsen which has an equivalent Polar Class rating of PC3. POLARIS recommends a speed limit of 5 knots, which is demonstrated to be insufficient to avoid the hazard by stopping.

iv. The size of a vessel will impact its manoeuvrability. A larger vessel will generally correspond to a larger stopping distance if the vessel speed is held constant. Thus, this implies that both vessel speed and physical parameters need to be considered in the assessment of safe navigation speed to ensure hazard avoidance.
v. Finally, as can be seen from some of the images, the increasing distortion of the images with distance from the camera suggests that it would be difficult to identify an ice hazard such as a multi-year ice floe, until it is closer to the vessel. This means that it is possible that the stopping distance and turning radius would not be sufficient to avoid ice impact for longer vessels or those travelling at higher speeds

CONCLUSIONS

The results presented in this paper show the possibility of using ship operational parameters, specifically speed, to demonstrate the varying manoeuvrability of a vessel, which will translate to its capability to avoid sea ice hazards. Additionally, image transformation and rescaling methods are illustrated and show great promise in being used for the augmentation of the sea ice field view with a vessel's specific manoeuvrability parameters. Key observations are made which highlight the limitations of POLARIS in sea ice hazard avoidance, as well as the importance of incorporation of vessel speed and physical parameters such as vessel length in the hazard avoidance assessment. The illustration of the boundaries of the stopping distance and the turning circle demonstrates a vessel's capabilities in sea ice and shows potential for onboard cameras being used as a support tool for ship operations in sea ice conditions.

FURTHER WORK

In this paper, the possibility of performing calculations to determine manoeuvrability parameters for specific vessels using operational parameters such as speed are shown and demonstrated. The practical implications of the data obtained from the methodologies illustrated in this work could be treated in a future paper.

ACKNOWLEDGEMENTS

I would like to acknowledge the contribution of Dr Rocky Taylor, Dr Tom Browne as well as Dr Ian Turnbull and Dr Oscar Desilva for their support guidance and assistance in carrying out the work demonstrated in this paper. Furthermore, I would also like to acknowledge Memorial University of Newfoundland, the National Research Council of Canada (NRC), the Natural Sciences and Engineering Research Council (NSERC) and the Hibernia Management and Development Company (HMDC) for their financial support. I further acknowledge the NRC for providing the data that was essential to this work.

REFERENCES

Bigg, Grant R., and Mattias Green. "*Has the impact of the Earth's orbital variation at sub-myriadal timescales been underestimated?"* (2023).

Kooij, Carmen, and Robert Hekkenberg. "*Towards unmanned cargo-ships: the effects of automating navigational tasks on crewing levels*." Available at SSRN 3438144 (2019).

Neville, M. A., F. Scibilia, and E. H. Martin. "*Physical Ice Management Operations-Field Trials and Numerical Modeling*." OTC Arctic Technology Conference. OTC, 2016.

Ruiz-De-Azúa, Joan A., Adriano Camps, and Anna Calveras Augé. "*Benefits of using mobile ad-hoc network protocols in federated satellite systems for polar satellite missions*." IEEE access 6 (2018): 56356-56367.

Randell, Charles, et al. "*SS: Canadian: Atlantic development; technological advances to assess, manage and reduce ice risk in northern developments.*" Offshore Technology Conference. OTC, 2009.

Zhou, Li, Jinyan Cai, and Shifeng Ding. "*The identification of ice floes and calculation of sea ice concentration based on a deep learning method*." Remote Sensing 15.10 (2023): 2663.

Browne, Thomas, et al. "*A framework for integrating life-safety and environmental consequences into conventional arctic shipping risk models*." Applied Sciences 10.8 (2020): 2937.

Transport Canada. 2019. *Guidelines for assessing ice operational risk*, TP NO. 15383E. March 2019

Sonka, Milan, Vaclav Hlavac, and Roger Boyle. *Image processing, analysis and machine vision.* Springer, {2013}.

Dubrofsky, Elan. "*Homography estimation*." Diplomová práce. Vancouver: Univerzita Britské Kolumbie 5 (2009).

Ammar Abbas, Syed, and Andrew Zisserman. "*A geometric approach to obtain a bird's eye view from an image*." Proceedings of the IEEE/CVF international conference on computer vision workshops. 2019.

Sandru, Andrei, et al. "*A complete process for shipborne sea-ice field analysis using machine vision*." IFAC-PapersOnLine 53.2 (2020): 14539-14545.

Imson, Grace. "*How to Calculate the Distance to the Horizon: Easy Formulas*." WikiHow, 23 May 2005, www.wikihow.com/Calculate-the-Distance-to-the-Horizon. Accessed 17 Feb. 2025.

American Bureau of Shipping. *Vessel Maneuverability*. 2006. Revised in 2017. Accessed 10 June 2024.